# DESIGN AND EXPERIMENTAL STUDY OF AN ADJUSTABLE WRAPPING MACHINE FOR RICE STRAW BALES OF DIFFERENT SIZES
# /
# 可调式秸秆包捆机的设计与试验研究

**Liyan WU[1)], Huchao TAN[2)], Na ZHANG[1)], Hengyi WEI[1)], Zhenyu WANG[1)], Chunhua BAN[3)], Cuihong LIU[*1)]**

[1)]College of Engineering, Shenyang Agricultural University, Shenyang / China
[2)]Yantai Taihai Manoir Nuclear Power Equipment Co., Ltd., Yantai / China
[3)]Liaoning Provincial Institute of Agricultural Mechanization / China
*Tel: +8615942060166; E-mail: cuihongliu77@syau.edu.cn*
*Corresponding author: Liu Cuihong*
*DOI: https://doi.org/10.35633/inmateh-76-36*

***Keywords:*** *rice straw; adjustable wrapping machine; straw bale; tensile film*

**ABSTRACT**

*China annually produces over 210 million tons of rice straw; however, its utilization as feed remains low due to the scarcity of supporting equipment. In feed production, wrapping straw bales with plastic film is crucial for accelerating degradation. Given the diverse types of straw balers, a variety of wrapping machines are required. This study presents the design of an adjustable wrapping machine capable of handling straw bales with diameters ranging from 400 to 1200 mm and lengths between 500 - 1000 mm. Wrapping time, coefficient of variation, and elongation rate were selected as key evaluation indicators. Experimental results demonstrate that all performance metrics comply with industry standards for straw bale machinery, indicating the machine's practical feasibility and reliability in agricultural applications.*

**摘要**

*中国水稻秸秆年产量在 2.1 亿吨以上，但饲料化利用率仍然很低，其原因是缺少配套的装备，饲料化生产需要利用塑料膜包裹稻草捆以加速降解。由于秸秆打包机类型较多，故此需要不同型号的包膜机与之相匹配。本工作设计了一种可调包装机，可实现直径 400~1200mm、长度 500~1000mm 的稻草捆进包膜处理。选取缠绕时间、变异系数和伸长率作为评价指标，通过包膜检验包膜效果。结果表明，各项指标均达到了秸秆包捆机械的行业标准。*

## INTRODUCTION

China boasts a colossal crop straw yield, with annual production reaching 800 million tons—equivalent to 30% of the global total, ranking first worldwide (*Tian, 2020; Cong et al., 2021; Zhang et al., 2021*). Among this, rice straw contributes 210 million tons yearly, accounting for approximately one - fourth of China's total crop straw resources *(Li et al., 2020; Lu et al., 2021; Liu, 2024*). However, current utilization methods (Fig. 1) remain inefficient. Burning straw for heat or char production results in low calorific value and causes environmental pollution. Returning straw to the soil offers limited economic benefits and increases the risk of pests. Industrial applications, such as the production of low-quality paper and rope, are hindered by high costs associated with collection, transportation, and labor (*Wang et al., 2017; Huo et al., 2019; Feng et al., 2021; Cong et al., 2019*). In contrast, feed utilization has emerged as a promising solution, offering economic benefits without causing environmental harm.

Nevertheless, raw rice straw is unpalatable and nutritionally inadequate for livestock, necessitating degradation and fermentation before being used as feed. Transforming rice straw into feed not only optimizes resource utilization (*Liu, 2021; Huo et al., 2022; Gu et al., 2017*) but also alleviates forage shortages, thereby benefiting animal husbandry.

In the rice straw feed production process, key steps include bundling, spraying decay agents, wrapping bales with plastic film, and fermenting. These treatments reduce crude fiber content while increasing protein and soluble sugar levels, thus boosting livestock feeding rates.

---

*Liyan Wu, Prof. Ph.D. Eng.; Huchao Tan, Na Zhang, Hengyi Wei, Zhenyu Wang, M.S. Stud. Eng.; Chunhua Ban, engineer; Cuihong Liu Prof. Ph.D. Eng.*

Commercially available wrapping machines struggle to accommodate straw bales of diverse sizes (with diameters ranging from 500 to 1200 mm and lengths from 500 to 1000 mm). In response, this study developed an adjustable wrapping machine compatible with various balers. Following tests and analysis of the mechanical properties of wrapping plastic films, the machine's structure was designed, and subsequent wrapping tests were conducted. Key parameters—including wrapping time, variation coefficient, and film elongation rate—were evaluated. These findings not only significantly enhance rice straw feed production efficiency but also provide valuable insights for the design of wrapping machinery for other crops and grasses.

## MATERIALS AND METHODS

Prior to designing the adjustable rice straw wrapping machine, a study on the mechanical characteristics of the tensile film was conducted. The test results will provide basic data for the subsequent determination of motion parameters, rotational speed, and the overall structural design of the machine.

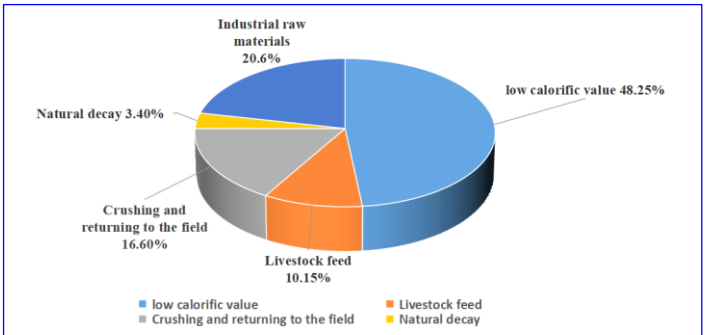


**Fig. 1 - Different utilization of rice straw**

*Materials and Instruments*

Tensile film: Antioxidant silage tensile film (thickness: 0.025 mm; width: 250 mm; material: linear low-density polyethylene (LLDPE)), produced by Shandong Xinlian Heavy Industry Agriculture and Animal Husbandry Machinery Company.

Test instrument: Universal material tensile testing machine. The sensor has a measuring range of 2 mN–2 kN with an accuracy of ±1% or better. The loading speed is adjustable within the range of 0.01–500 mm/min.

*Methods*

The operation process includes 5 steps: sample preparation, length and width determination, calibration, testing, and data processing. A quadratic orthogonal rotation combination test scheme was adopted, with tensile film length ($X_1$), width ($X_2$), and loading speed ($X_3$) set as the test factors. According to the test requirements, the levels of the test factors are represented by the coded values -1.628, -1, 0, 1, and 1.628. The corresponding relationship between the coded values and actual values of the test scheme is shown in Table 1.

**Table 1**

**Factor level coding**

| Levels | Factors | | |
|---|---|---|---|
| | Length $X_1$/(mm) | Stretch film width $X_2$/(mm) | Loading speed $X_3$/ (mm/min) |
| -1.682 | 70 | 18 | 60 |
| -1 | 100 | 23 | 75 |
| 0 | 150 | 30 | 100 |
| 1 | 200 | 37 | 125 |
| 1.682 | 230 | 42 | 140 |

In accordance with the national standards "Determination of Tensile Properties of Plastic Films" (GB/T 13022-91) and "Test Conditions for Films and Sheets in the Determination of Plastic Tensile Properties" (GB/T 1040-2006), the maximum tensile force (Y1) and elongation at break (Y2) were designated as the test indicators. Tensile film samples were cut neatly, as illustrated in Fig. 2.

Y1, the maximum force at which the film breaks.

$\varepsilon_t$, elongation rate calculated by Equation (1).

$$\varepsilon_t = \frac{L - L_0}{L_0} \times 100\% \quad (1)$$

where:

$L_0$—original length of the tensile film, [mm];

$L$—length after breaking, [mm].

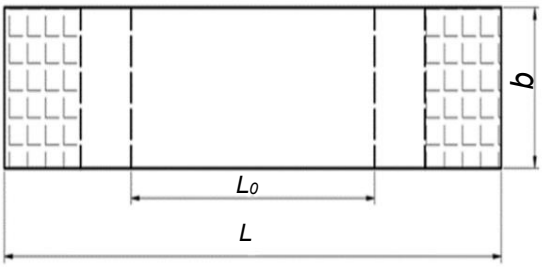


**Fig. 2 - Tensile test device**

## RESULTS AND ANALYSIS

### *Establishment of tensile film model*

Using Design-Expert 12.0 software, an analysis of the test factors and indicators was conducted to determine the influence of each factor. The test scheme and corresponding results are presented in Table 2.

**Table 2**

**Test scheme and results**

| Test number | Test factors | | | Test indicators | |
|---|---|---|---|---|---|
| | Mold length X1 / (mm) | Film width X2 / (mm) | Loading speed X3 / (mm/s) | Maximum breaking force Y1 / (N) | Elongation rate Y2 / (%) |
| 1 | -1 | -1 | -1 | 16.2 | 262.7 |
| 2 | 1 | -1 | -1 | 12.6 | 212.1 |
| 3 | -1 | 1 | -1 | 21.1 | 283.4 |
| 4 | 1 | 1 | -1 | 16.4 | 253.7 |
| 5 | -1 | -1 | 1 | 10.8 | 257.1 |
| 6 | 1 | -1 | 1 | 9.3 | 214.8 |
| 7 | -1 | 1 | 1 | 18.3 | 239.8 |
| 8 | 1 | 1 | 1 | 16.8 | 232.1 |
| 9 | -1.682 | 0 | 0 | 18.5 | 286.4 |
| 10 | 1.682 | 0 | 0 | 12.8 | 205.4 |
| 11 | 0 | -1.682 | 0 | 10.1 | 209.1 |
| 12 | 0 | 1.682 | 0 | 21.4 | 265.2 |
| 13 | 0 | 0 | 1.682 | 11.8 | 276.5 |
| 14 | 0 | 0 | -1.682 | 10.5 | 230.1 |
| 15 | 0 | 0 | 0 | 11.3 | 242.3 |
| 16 | 0 | 0 | 0 | 10.7 | 236.1 |
| 17 | 0 | 0 | 0 | 10.6 | 246.4 |
| 18 | 0 | 0 | 0 | 11.7 | 239.6 |
| 19 | 0 | 0 | 0 | 10.9 | 232.1 |
| 20 | 0 | 0 | 0 | 10.3 | 231.6 |
| 21 | 0 | 0 | 0 | 11.5 | 234.1 |
| 22 | 0 | 0 | 0 | 10.3 | 235.9 |
| 23 | 0 | 0 | 0 | 9.9 | 227.4 |

### *Establishment of regression model of the maximum breaking force*

The regression equation composed of primary, quadratic and interaction terms are obtained, equation (2). This regression equation expressed the relationship of the maximum breaking force Y1 and the three factors, the film length X1, width X2, and the loading speed of X3.

$$\hat{Y_1} = 10.78 - 1.53X_1 + 3.13X_2 - 0.97X_3 + 0.66X_1X_3 + 0.79X_2X_3 = 1.88{X_1}^2 + 1.92{X_2}^2 \quad (2)$$

The significance of the regression equation was tested using ANOVA, and the results are presented in Table 3.

**Table 3**

**Variance analysis of experiment results $Y_1$**

| Variance source | Square sum | Degrees of freedom | Mean square | F-value | P-value |
|---|---|---|---|---|---|
| Mold | 301.84 | 9 | 33.54 | 47.30 | < 0.0001** |
| $X_1$ | 31.94 | 1 | 31.94 | 50.45 | < 0.0001** |
| $X_2$ | 133.53 | 1 | 133.53 | 188.33 | < 0.0001** |
| $X^3$ | 12.93 | 1 | 12.93 | 18.23 | 0.0009** |
| $X_1X_2$ | 0.15 | 1 | 0.15 | 0.21 | 0.6518 |
| $X_1X_3$ | 3.51 | 1 | 3.51 | 4.95 | 0.0444* |
| $X_2X_3$ | 4.96 | 1 | 4.96 | 7.00 | 0.0202* |
| $X_1^2$ | 56.18 | 1 | 56.18 | 79.24 | < 0.0001** |
| $X_2^2$ | 58.32 | 1 | 58.32 | 82.25 | < 0.0001** |
| $X_3^2$ | 1.33 | 1 | 1.33 | 1.68 | 0.1939 |
| Residual | 9.22 | 13 | 0.71 | | |
| Lost proposal | 6.30 | 5 | 1.26 | 3.45 | 0.0869 |
| Error term | 2.92 | 8 | 0.36 | | |
| Aggregate | 311.06 | 22 | | | |

Note: * * Most significant level (p <0.01); * significant level (p <0.05).

As showed in Table 3, the established model is highly significant ($P < 0.0001$), the P-values of the three factors $X_1$, $X_2$, $X_3$ are less than 0.05, indicate that each factor exerts a significant effect on the maximum breaking force. The lack-of-fit term (P=0.0869)>0.05) is non-significant, demonstrating that the model has a high degree of reliability. The order of influence of the three factors on the maximum breaking force is $X_2>X_1>X_3$. i.e., tensile film width> tensile film length > loading speed. Specifically:

The linear terms $X_1$, $X_2$ and $X_3$ have highly significant effects on the results ($P < 0.01$).

The interaction terms $X_1X_3$ and $X_2X_3$ exert significant effects ($p < 0.05$), while the interaction term $X_1X_2$ has a non-significant effect ($p > 0.05$).

The quadratic terms $X_1^2$ and $X_2^2$ show highly significant effects ($p < 0.01$), whereas the quadratic term $X_3^2$ has a non-significant effect ($p > 0.05$).

***Establishment of regression model of the elongation rate***

Through fitting the test results using Design-Expert 12.0 software, a regression equation incorporating linear terms, quadratic terms, and interaction terms was derived, as shown in Equation (3). This regression equation characterizes the relationship between the elongation ($Y_2$) and the three factors: tensile film length ($X_1$), width ($X_2$), and loading speed ($X_3$).

$$\hat{Y_2} = 238.08 - 19.52X_1 + 11.47X_2 - 10.70X_3 + 6.94X_1X_2 + 7.79X_2X_3 + 5.71{X_3}^2 \quad (3)$$

This regression equation is tested with ANOVA, and the results are shown in Table 4.

**Table 4**

**Variance analysis of $Y_2$**

| Variance source | Square sum | Degrees of freedom | Mean square | F-value | P-Value |
|---|---|---|---|---|---|
| Mold | 10121.78 | 9 | 1124.64 | 18.93 | < 0.0001** |
| $X_1$ | 5201.47 | 1 | 5201.47 | 78.67 | < 0.0001** |
| $X_2$ | 1796.81 | 1 | 1796.81 | 27.17 | 0.0010** |
| $X_3$ | 1563.72 | 1 | 1563.72 | 23.65 | 0.0003** |
| $X_1X_2$ | 385.03 | 1 | 385.03 | 5.82 | 0.0313* |
| $X_1X_3$ | 114.76 | 1 | 114.76 | 1.74 | 0.2104 |
| $X_2X_3$ | 485.16 | 1 | 485.16 | 7.34 | 0.0179* |
| $X_1^2$ | 154.65 | 1 | 154.65 | 2.34 | 0.1501 |
| $X_2^2$ | 110.11 | 1 | 110.11 | 1.64 | 0.8900 |
| $X_3^2$ | 522.79 | 1 | 522.79 | 7.91 | 0.0147* |
| Residual | 859.58 | 13 | 66.12 | | |
| Lost proposal | 586.66 | 5 | 117.37 | 3.44 | 0.0590 |
| Error term | 272.72 | 8 | 34.09 | | |
| Aggregate | 11080.08 | 22 | | | |

Note: * * Most significant level (p <0.01); * significant level (p <0.05).

As can be seen from Table 4, the established model is significant ($P < 0.0001$), the P-value of the three factors X1, X2, X3 are all less than 0.05, indicating that the three factors have a significant impact on the elongation. The lack of fit term (P(0.059)>0.05) is not significant, which suggests that the model has a high degree of reliability. The order of influence of the three factors on the elongation Y2 is X1 > X2 > X3, i.e., the film length X1 > width X2 > loading speed X3. Specifically:

The linear terms (primary terms) X1, X2, and X3 all have a highly significant effect on the results (P < 0.01).

The interaction terms X1X2 and X2X3 have a significant effect (P < 0.05), while the interaction term X1X3 has no significant effect (P > 0.05).

The quadratic term (secondary term) X3 has a significant effect on the results (P < 0.05), whereas the quadratic terms X1 and X2 have no significant effect (P > 0.05).

***Overall structure of the machine***

The adjustable wrapping machine is designed for wrapping rice straw bales of varying sizes, consisting primarily of a frame, an adjustable roller mechanism, a rocker mechanism, a film-supplying mechanism, a lifting mechanism, and a transmission system. The adjustable roller, rocker mechanism, and transmission system are all motor-driven.

The adjustable roller mechanism is mainly composed of two rollers and a circulating reciprocating drive device, where the latter consists of a stepper motor, left- and right-hand screws, rails, and sliding blocks. This mechanism is capable of lifting straw bales with diameters ranging from 500 to 1200 mm. The transmission system drives the rollers to rotate the straw bale.

The rocker mechanism comprises a rocker arm, a frame, and a gear motor. The overall structure of the adjustable straw bale wrapping machine is illustrated in Fig. 3.

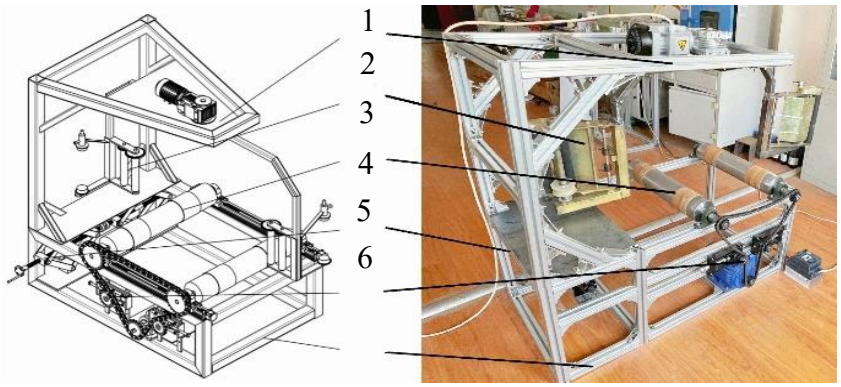


**Fig. 3 - The overall structure of the machine**

*1- Rocker mechanism; 2-Film supplying mechanism; 3-Adjustable roller mechanism; 4-Lifting mechanism; 5-Chain tensioning mechanism; 6-Frame*

***Working principle***

Before operation, the distance between the two rollers is adjusted to an appropriate position by moving the sliding blocks according to the size of the straw bale. The straw bale is then placed on the supporting rollers. Via the lifting mechanism, the symmetrical center plane of the film-feeding mechanism is aligned with the center plane of the straw bale. Subsequently, the tensile film is threaded through the film-feeding rollers, preparing for the wrapping process.

During operation, the sprocket motor is activated to rotate the rollers, which in turn drives the straw bale to rotate around its axis. Simultaneously, the rocker mechanism is initiated, carrying the film-supplying mechanism to revolve around the straw bale. The tensile film is fed through the film-supplying rollers and exits with a certain degree of tension and elongation. Through the combined rotation of the straw bale and the rocker arm, the plastic film is wrapped around the bale.

In the wrapping process, the film-supplying mechanism and the straw bale rotate simultaneously, with their respective rotation planes perpendicular to each other. For each full rotation of the film, the straw bale rotates by a corresponding angle. When the tensile film completes its second rotation, it overlaps with the first rotation by a certain extent; this rotation continues until the wrapping process is finished.

For each batch of straw bales of the same size, the roller spacing and height only need to be adjusted once to meet operational requirements. The overall design of the machine complies with the standard DB21/T 3527-2021, featuring simple operation, a compact structure, and low noise. Relevant parameters of the machine are listed in Table 5.

**Table 5**

**Main parameters of the whole machine**

| Name | Parametric |
|---|---|
| Mass / kg | 380 |
| Sizes / mm | 1580×1140×1780 |
| Drive method | Electric powered |
| Round bale size (Diameter×Length) | Φ500×500~Φ1200×1000 |
| Number of film layers/layer | ≧2 |
| Operating efficiency/(pack/h) | 50 |
| Bunching rate /% | ≧99 |

***Theoretical analysis of the wrapping process***

***Force analysis of the wrapping process***

During the wrapping process, the straw bale is subjected to several forces: its own gravity G, the tension from the tensile film $F_{pull}$, the normal support forces from the two rollers $F1$, $F2$, and the frictional forces between the rollers and the bale surface $f_1, f_2$ (*Li et al.,2018*), as illustrated in Fig.4.

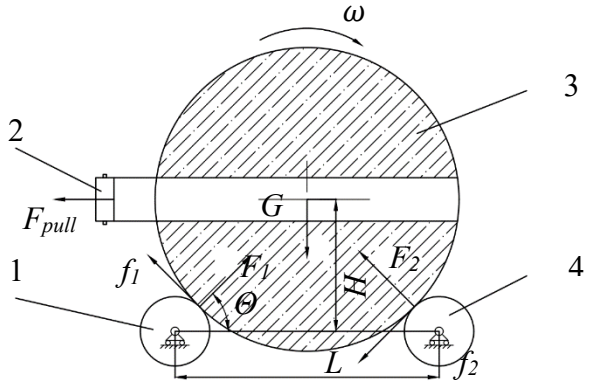


**Fig. 4 - Stress analysis diagram of straw bale**

*1-Left roller; 2-Film roller; 3-Straw bale; 4-Right roller*

The tensile force of the film significantly affects the quality and stability of the wrapping effect. Excessive tensile force can easily cause the straw bale to become unbalanced and roll. In such cases, the normal support force of the right roller becomes zero, and the frictional force between the right roller and the straw bale also vanishes. It is therefore necessary to analyze the forces acting on the bale in this critical state, as expressed in Equation (4) below:

$$F_{pull}L_1 = F_1\frac{L_1}{2}cos\,\theta - f_1\frac{L_1}{2}sin\,\theta \tag{4}$$

In Fig.4:

$$G = F_1\,sin\,\theta \tag{5}$$

$$f_1 = \mu F_1 \tag{6}$$

where:

$F_{pull}$— The pulling force exerted by the film on the straw bale, [N];

$G$— Gravity, [N];

$F_1$—The normal support force of the left roller, [N];

$f_1$—The friction between the left roller and the straw bale, [N];

$L_1$—The length of the straw bale, [mm];

$\mu$—The coefficient of friction between the left roller and the straw bale;

$\theta$—The angle between $F_1$ and the horizontal direction, [°].

From the above equation, it can be seen that in the process of wrapping, the $F_{pull}$ should satisfy the following equation (7):

$$F_{pull} \le \frac{G}{2}(cot\theta - \mu) \tag{7}$$

Furthermore, based on equations from (4) to (6), the $F_{pull}$ is related to the gravity of the bale, the friction coefficient between the bale and the rollers, and the angle between the support force and the horizontal line. For the maximum bale size is selected, its weight is approximately 72 kg. When the angle is 45°, the straw bale rotates most smoothly on the roller. With a friction coefficient of 0.78, the calculated $F_{pull}$ value is 79.2N. Therefore, to ensure the smooth rotation of the straw bale during the wrapping process, the tensile force exerted by the film on the bale should be less than 79.2 N.

***Determination of the speed ratio (i)***

The overlap rate directly affects the quality of wrapping, fermentation efficiency, storage duration, and compactness of straw bales. Theoretically, more wrapping layers improve fermentation outcomes (*Zhang et al., 2017*), but in practical production, 2 layers of tensile film are sufficient to ensure effective fermentation. In this experiment, wrapping tests with 2, 4, and 6 layers of film were conducted to analyze film elongation performance and wrapping efficiency.

The overlap rate must be set reasonably: an excessively low rate results in poor sealing, which can easily lead to fermentation failure; while an excessively high rate, although ensuring good sealing, may cause film waste and significantly reduce efficiency. In this study, the film overlap rate was set at 50%, meaning each cycle of film covers half of the area wrapped in the previous cycle (*Zhang et al., 2019; Wang et al., 2024*). A schematic diagram of the overlap effect is shown in Fig. 5.

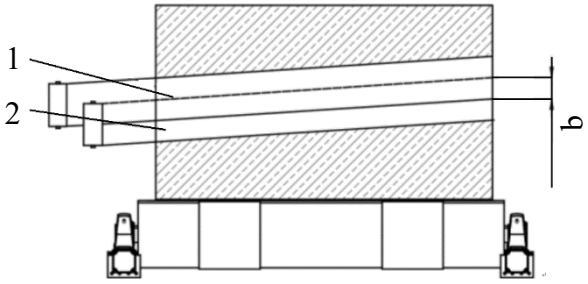


**Fig. 5 - Overlapping diagram of straw bale**

*1 - First film; 2 - Second film*

The overlap coefficient M of the tensile film can be calculated by Equation (8):

$$M = \left(\frac{b_1 - b}{b_1}\right) \times 100\% \tag{8}$$

And the following equations:

$$b = \omega r t \tag{9}$$

$$\omega = \frac{2\pi n_1}{60} \tag{10}$$

$$t = \frac{60}{n_2} \tag{11}$$

where:

$M$—Overlap coefficient of the tensile film, 50 %;

$b_1$—Width of the tensile film, 250 mm;

$b$—Staggered distance between two adjacent films, [mm];

$\omega$—Angular speed of the roller, [rad/s];

$r$—Roller radius, 80 mm;

$t$—Time for the rocker to rotate around the bale, [s];

$n_1$—Roller speed, [r/min];

$n_2$—Rotational speed of the rocker, [r/min].

By substituting Equations (9) ~ (11) into Equation (8), M can be calculated using Equation (12).

$$M = \left(1 - \frac{2n_1}{n_2}\right) \times 100\% \tag{12}$$

Wrapping efficiency is determined by the roller speed and rocker speed. When the overlap rate (M) is 50%, the calculated speed ratio between the roller and the rocker arm ($n_1/n_2$) is approximately 0.25, which provides a basis for the design of the transmission mechanism.

## DESIGN OF THE KEY COMPONENTS OF THE WHOLE MACHINE

### *Design of the adjustable roller mechanism*

The adjustable roller mechanism, as illustrated in Fig. 6, mainly consists of two rollers, a stepper motor, a guideway, a sliding plate, a coupling, left- and right-hand threaded rods, and a limit block. During the wrapping process, the straw bale is placed on the two rollers, and the adjustable roller mechanism allows for the placement of straw bales with different diameters. In this study, the distance between the two rollers can be adjusted within the range of 466 mm to 960 mm to accommodate straw bales of varying sizes.

The two rollers are fixed to the ends of the sliding plates via bearing blocks. While the rollers drive the straw bale to rotate, the stepper motor drives the threaded rods to rotate, enabling the symmetrical movement of the sliding blocks.

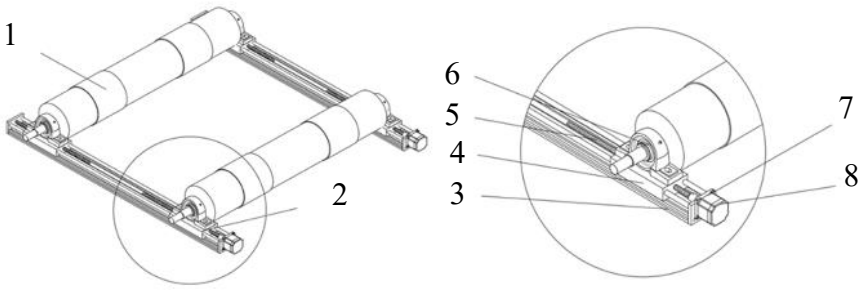


**Fig. 6 - Structure diagram of adjustable rice straw bale wrapping machine**
*1 - Roller; 2 - Reciprocating drive; 3 - Guideway 4 - Slider; 5 - Left and right rotating screws; 6 - Rolling bearing; 7 - Limit switch; 8 - Stepper motor*

### *Design of the film supply mechanism*

The film supply mechanism is mounted on the rocker arm (*Yang et al., 2020; Zhao et al., 2024*), consisting of upper and lower support rollers, two film supply rollers, a supply frame, a torsion spring, a film baffle, a sprocket, and a film roll. Its structure is illustrated in Fig. 7. The film is secured between the upper and lower support rollers, with the two film supply rollers positioned on the supply frame. The two film supply rollers are driven by a sprocket, which pulls the tensile film from the film roll.

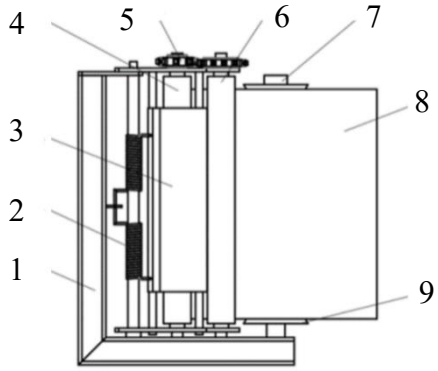


**Fig. 7 - Schematic diagram of the film supplying mechanism**
*1 - Frame; 2 - Torsion spring; 3 - Baffle 4 - Supply rollers 5 - Sprocket; 6 - Supply rollers; 7 - Upper supporting roller; 8 - Film; 9 - Lower supporting roller*

### *Rocker arm mechanism design*

The rocker mechanism is primarily responsible for supporting the rocker arm and motor, while driving the rocker arm and film-supplying mechanism to rotate around the straw bale. Composed of a rocker arm, support frame, motor, and fixing plate (as shown in Fig. 8), the mechanism features a rocker motor connected to the middle of the rocker arm. The lower part of the rocker arm is positioned facing the adjustable roller mechanism, with its rotation center aligned with the symmetric central plane of the adjustable roller mechanism. This design prevents eccentricity.

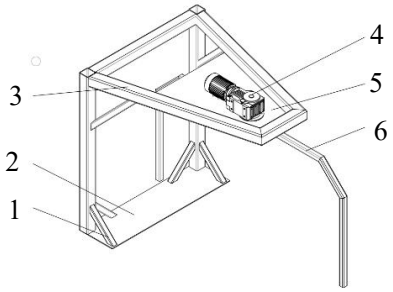


**Fig. 8 - Schematic diagram of rocker arm mechanism**

*1 - Stiffener; 2 - Fixed base plate; 3 - Rocker racks; 4 - Rocker motor; 5 - Motor fixing plate; 6. Rocker*

## PERFORMANCE TEST OF ADJUSTABLE RICE STRAW ROUND BALE WRAPPING MACHINE

Materials: Three sizes of rice straw bundles (400×400 mm, 500×500 mm, 600×600 mm) with good compaction were used in the test. All bundles were well compacted, free from protrusions or sharp edges, and had an average moisture content of 55%. Tensile film: The wrapping film used was linear low-density polyethylene (LLDPE) with a thickness of 0.025 mm and a width of 250 mm. It was supplied by Shandong Xinlian Heavy Industry Agriculture and Animal Husbandry Machinery Co., Ltd.

Methods: In accordance with the standards DB21/T 3527–2021 and NY/T 3121–2017, straw bales were divided into three groups by size (400×400 mm, 500×500 mm, 600×600 mm). Wrapping tests with 2, 4, and 6 layers of film were conducted for each group, with the following evaluation indicators:

Wrapping time

Defined as the time required to wrap a single straw bale. Five replicate tests were performed, and the average value was calculated.

Coefficient of variation of layers

For each bale size, 5 bales were randomly selected. At 5 randomly chosen positions on each bale, the tensile film was cut along the circumferential direction, and the average number of film layers at these 5 positions was recorded.

Elongation rate

Marker holes were punched in the middle of the film roll, with tracers inserted into the holes as reference marks. After wrapping, the positions of these marker holes were identified on the bale surface, and the distance between two adjacent holes was measured as L. The elongation rate ($\varepsilon_t$) was then calculated using Equation (13):

$$\varepsilon_t = \frac{L - L_0}{L_0} \times 100\% \quad (13)$$

where:

$L$ is the distance between two marking holes after wrapping operation, and $L_0$ is actually the circumference of the film roll.

The rocking arm mechanism speed was set to 35 r/min, as referenced by *Yang, (2016)*. Based on the transmission ratio between the roller and the rocker arm (i = 0.25), the corresponding roller speed was calculated to be 8.75 r/min. The spacing between the two rollers was adjusted according to the size of the straw bale: 353 mm for 400×400 mm bales, 424 mm for 500×500 mm bales, and 495 mm for 600×600 mm bales.

## RESULTS AND ANALYSIS

### *Wrapping time*

The test results are presented in Table 6. Wrapping time varies depending on the specifications of the straw bales:

For 400×400 mm bales, the average wrapping times for 2, 4, and 6 layers were 18.6 s, 32.4 s, and 44.8 s, respectively.

For 500×500 mm bales, the average wrapping times for 2, 4, and 6 layers were 20.4 s, 33.6 s, and 45.2 s, respectively.

For 600×600 mm bales, the average wrapping times for 2, 4, and 6 layers were 21.4 s, 34.4 s, and 46.4 s, respectively.

All results meet the industry standards for straw bale wrapping machinery.

**Table 6**

**Wrapping time of straw bales with different sizes**

| Number of wrapping layer | 400×400 mm wrapping time /s | | | | | |
|---|---|---|---|---|---|---|
| | 1 | 2 | 3 | 4 | 5 | Average value |
| **2** | 18 | 19 | 18 | 19 | 19 | 18.6 |
| **4** | 33 | 32 | 33 | 32 | 32 | 32.4 |
| **6** | 44 | 44 | 46 | 45 | 45 | 44.8 |
| **Number of wrapping layer** | **500×500 mm wrapping time /s** | | | | | |
| | 1 | 2 | 3 | 4 | 5 | Average value |
| **2** | 19 | 21 | 20 | 21 | 21 | 20.4 |
| **4** | 33 | 33 | 34 | 33 | 35 | 33.6 |
| **6** | 45 | 45 | 46 | 45 | 45 | 45.2 |
| **Number of wrapping layer** | **600×600 mm wrapping time /s** | | | | | |
| | 1 | 2 | 3 | 4 | 5 | Average value |
| **2** | 21 | 21 | 21 | 22 | 22 | 21.4 |
| **4** | 34 | 35 | 34 | 34 | 35 | 34.4 |
| **6** | 46 | 47 | 47 | 46 | 46 | 46.4 |

***Coefficient of variation of layers***

Fifteen groups of tests were conducted, with forty-five points randomly selected to record the number of film layers. The results are presented in Table 7. All 15 groups showed a film overlap rate exceeding 50%, and the number of layers at each point was calculated using Equation (14).

$$C = \frac{C_1 + C_2 + C_3 + \cdots C_{45}}{45} = \sum_{i}^{45} C_i/45 \tag{14}$$

where:

$C$—Average value of layers.

$C_i$—$C_1 \cdots C_{45}$ Number of layers at each point.

The coefficient of variation is calculated using Equation (15).

$$X = \frac{S}{C} \times 100\% \tag{15}$$

where: S is the standard deviation calculated by Equation (16).

$$S = \sqrt{\frac{\sum_i^{45}(C_i - C)^2}{45 - 1}} \tag{16}$$

After calculation, the coefficients of variation for the uniformity of the wrapping film were found to be 8.70% (400×400 mm), 11.20% (500×500 mm), and 10.70% (600×600 mm), respectively. All these values are below the 15% threshold specified in the industry standards for straw bale wrapping machinery.

**Table 7**

**Number of wrapping film pickup points for different straw bale sizes and layer counts**

| Straw bale specifications | Straw bale number | 2-layer film pickup point number | | | | | 4-layer film pickup point number | | | | | 6-layer film pickup point number | | | | |
|---|---|---|---|---|---|---|---|---|---|---|---|---|---|---|---|---|
| | | 1 | 2 | 3 | 4 | 5 | 1 | 2 | 3 | 4 | 5 | 1 | 2 | 3 | 4 | 5 |
| 400×400mm Straw bale | 1 | 2 | 2 | 2 | 2 | 2 | 4 | 4 | 4 | 4 | 4 | 6 | 6 | 6 | 6 | 6 |
| | 2 | 2 | 2 | 2 | 2 | 2 | 4 | 3 | 4 | 4 | 4 | 7 | 6 | 6 | 6 | 6 |
| | 3 | 2 | 3 | 2 | 2 | 2 | 4 | 4 | 4 | 5 | 4 | 6 | 6 | 6 | 5 | 6 |
| | 4 | 2 | 2 | 2 | 2 | 2 | 4 | 5 | 4 | 4 | 4 | 6 | 6 | 6 | 6 | 6 |
| | 5 | 2 | 2 | 2 | 2 | 3 | 4 | 4 | 4 | 4 | 4 | 6 | 6 | 6 | 6 | 6 |
| 500×500mm Straw bale | 1 | 2 | 2 | 2 | 2 | 2 | 4 | 4 | 4 | 4 | 4 | 6 | 6 | 6 | 6 | 6 |
| | 2 | 2 | 2 | 3 | 2 | 2 | 4 | 4 | 5 | 4 | 4 | 6 | 5 | 6 | 6 | 6 |
| | 3 | 2 | 2 | 2 | 2 | 2 | 4 | 4 | 4 | 4 | 4 | 6 | 6 | 6 | 6 | 6 |
| | 4 | 2 | 2 | 2 | 2 | 2 | 4 | 4 | 4 | 5 | 4 | 6 | 6 | 5 | 6 | 6 |
| | 5 | 2 | 2 | 2 | 2 | 2 | 4 | 4 | 4 | 4 | 4 | 6 | 6 | 6 | 6 | 6 |

| Straw bale specifications | Straw bale number | 2-layer film pickup point number | | | | | 4-layer film pickup point number | | | | | 6-layer film pickup point number | | | | |
|---|---|---|---|---|---|---|---|---|---|---|---|---|---|---|---|---|
| | | 1 | 2 | 3 | 4 | 5 | 1 | 2 | 3 | 4 | 5 | 1 | 2 | 3 | 4 | 5 |
| 600×600mm Straw bale | 1 | 2 | 2 | 2 | 2 | 2 | 4 | 4 | 5 | 4 | 4 | 6 | 6 | 7 | 6 | 6 |
| | 2 | 2 | 2 | 3 | 2 | 2 | 4 | 4 | 4 | 4 | 4 | 6 | 6 | 6 | 6 | 6 |
| | 3 | 2 | 2 | 2 | 2 | 2 | 4 | 4 | 5 | 4 | 4 | 6 | 6 | 6 | 7 | 6 |
| | 4 | 2 | 2 | 3 | 2 | 2 | 4 | 4 | 4 | 4 | 4 | 6 | 6 | 6 | 6 | 6 |
| | 5 | 2 | 2 | 2 | 2 | 2 | 4 | 4 | 4 | 4 | 4 | 6 | 6 | 6 | 6 | 6 |

***Elongation rate $\varepsilon_t$***

Five wrapped bales of each size were randomly selected, and the elongation rate ( $\varepsilon_t$) was calculated using Equation (13). The final result was approximately 59%, with a 2.4% deviation from the design requirements. This elongation rate meets the industry standard, and detailed results are presented in Table 8.

**Table 8**

**Elongation rate**

| Measured parameter | Elongation of 5 tested wrapping bales - 400×400mm | | | | | |
|---|---|---|---|---|---|---|
| | 1 | 2 | 3 | 4 | 5 | Average value |
| $L_0$(mm） | 315.8 | 312.6 | 310.1 | 307.4 | 304.3 | 310.04 |
| $L_1$(mm) | 496.1 | 491.7 | 498.6 | 487.5 | 484.7 | 491.72 |
| $\varepsilon_t$ | (491.72-310.04)/310.14×100%=59% | | | | | |
| **Measured parameter** | **Elongation of 5 tested wrapping bales - 500×500mm** | | | | | |
| | 1 | 2 | 3 | 4 | 5 | Average value |
| $L_0$(mm） | 329.1 | 326.9 | 323.7 | 320.9 | 318.6 | 323.84 |
| $L_1$(mm) | 519.6 | 525.0 | 511.7 | 504.8 | 507.2 | 513.66 |
| $\varepsilon_t$ | (513.66-323.84)/323.84×100%=59% | | | | | |
| **Measured parameter** | **Elongation of 5 tested wrapping bales - 600×600mm** | | | | | |
| | 1 | 2 | 3 | 4 | 5 | Average value |
| $L_0$(mm） | 341.3 | 338.9 | 336.2 | 333.4 | 331.7 | 336.3 |
| $L_1$(mm) | 539.3 | 539.5 | 544.6 | 529.4 | 528.1 | 536.18 |
| $\varepsilon_t$ | (536.18-336.3)/336.3×100%=59% | | | | | |

## CONCLUSIONS

In the entire process of rice straw forage production, straw bales require wrapping, but the supporting machinery cannot adapt to bales of different sizes. To address this issue, this study designed a rice straw bale wrapping machine with adjustable rollers to accommodate various bale sizes, laying a foundation for improving the production efficiency of straw forage. The main conclusions are as follows:

(1) The mechanical properties of stretch films were studied. Film length, width, and loading speed were selected as test factors, with maximum tensile force and elongation rate as evaluation indicators. The results indicate that in actual wrapping operations, using shorter film lengths, lower loading speeds, and wider film widths can not only enhance the tensile strength of the film but also increase its elongation, thereby improving wrapping effectiveness.

(2) The overall structural scheme of the adjustable straw bale wrapping machine was designed. Based on theoretical analysis of the wrapping process, the tension applied to straw bales should be less than 79.2 N. A speed ratio of 0.25 between the roller and the rocker arm ensures a 50% wrapping overlap rate, achieving optimal wrapping results.

(3) Key components including the adjustable roller mechanism, film feeding mechanism, and rocker mechanism were designed. The spacing between the two rollers can be adjusted within the range of 466–960 mm, enabling the wrapping of bales with sizes ranging from 400 to 1200 mm.

(4) Performance testing of the adjustable straw bale wrapping machine was completed, with the rocker speed set at 35 r/min. The average wrapping times for 2, 4, and 6 layers of different-sized bales were measured. The film overlap rate reached 50%, with coefficients of variation for film uniformity at 8.70%, 11.20%, and 10.70% respectively, and the total average elongation rate of the stretch film was 59%. All indicators meet the design standards.

**ACKNOWLEDGEMENT**

This research was supported by the National Key Research and Development Program of China (2023YFD2301605). Key Research and Development Program of Liaoning province, China (2024JH2/102500004).

**REFERENCES**

[1] Cong, H., Meng, H., Yu, J., Ye, B., Yao, Z., Feng, J., Yu, B., Qin, C., Huo, L., Yuan, Y., Dai, M., Li, L., Shen, Y., Zhao, L., (2021). Analysis of the long-term mechanism of straw industry development in Northeast China under the guidance of "green" ("绿色"引领下东北地区秸秆产业发展长效机制解析). *Journal of Agricultural Engineering*, Vol. 37, pp. 314-321, Beijing/China.

[2] Cong, H., Yao, Z., Zhao, L., Meng, H., Wang, J., Huo, L., Yuan, Y., Jia, J., Xie, T., Wu, Y., (2019), The distribution of crop straw resources and their industrial system and utilization path in China (中国农作物秸秆资源分布及其产业体系与利用路径). *Journal of Agricultural Engineering*, Vol. 35, pp. 132-40, Beijing/China.

[3] Feng, P., Wu, H., Meng, F., Zheng, H., Yang, Z., Wang, J., Shen, Z., (2021). Effect of different compatible biological agents on the silage quality and feeding value of rice straw (不同配伍生物制剂对水稻秸秆青贮品质及饲喂价值的影响). *China Feed*, Vol. 17, pp. 122-128, Beijing/China.

[4] Gu, Y., Zhan, J., Ding, C., Sha, W., (2017). Effect of different treatments on the fermentation quality of fermented rice straw (不同处理对发酵稻秸秆发酵品质的影响). *China Feed*, Vol. 12, pp. 18-20 + 23, Beijing/China.

[5] Huo, L., Yao, Z., Zhao, L., Luo, J., Zhang P., (2022), Research on the contribution and potential of emission reduction and carbon sequestration in the comprehensive utilization of straw (秸秆综合利用减排固碳贡献与潜力研究). *Journal of Agricultural Machinery*, Vol. 53, pp. 349-359, Beijing/China.

[6] Huo, L., Zhao, L., Meng, H., Yao, Z., (2019). Study on the comprehensive utilization potential of crop straw in China (中国农作物秸秆综合利用潜力研究). *Journal of Agricultural Engineering*, Vol. 35, pp. 218-224, Beijing/China.

[7] Li, L., Wang, D., Yang, X., (2018). Study on round rice straw bale wrapping silage technology and facilities [J]. *Int J Agric & Biol Eng*, Vol. 11, pp. 88-95, Beijing/China.

[8] Li, S., Ji, X., Deng, K., Zhu, J., Li, C., Jian, Y., Peng, H., (2020). Analysis of regional straw resources distribution and full quantitative utilization potential (区域秸秆资源分布及全量化利用潜力分析). *Journal of Agricultural Engineering*, Vol. 36, pp. 221-228, Beijing/China.

[9] Liu, M., (2021). Application of Aspergillus Niger in the resourcable utilization of straw. *IOP Conference Series: Earth and Environmental Science*, Vol. 859, pp. 012092, England.

[10] Liu, Y., (2024). Research status and development trend of large square baler (大方捆打捆机的研究现状与发展趋势). *Xinjiang Agricultural Mechanization*, Vol. 06, pp. 54-57, Xinjiang/China.

[11] Lu, H., Chen, Y., Zhang, P., Huan, H., Xie, H, Hu, H., (2021). Impacts of farmland size and benefit expectations on the utilization of straw resources: Evidence from crop straw incorporation in China. *Soil Use and Management*, Vol. 38, pp. 929-939, England.

[12] Tian, Y., (2020). Research on the industry promotion policy of the comprehensive utilization of crop straw in China (我国农作物秸秆综合利用产业促进政策研究). *Agricultural Resources and regionalization*, Vol.41, pp. 28-36, Beijing/China.

[13] Wang, J., Li, X., Huang, W., Wu, L., Cui, J., Bai, H., Zeng, F. (2024). Mathematical model for bale-density prediction in large steel roller-type round balers during bale rolling. *Bioresource technology*. Vol. 396, England.

[14] Wang, J., Tang, H., Wang, J. (2017). Analysis on the comprehensive utilization status and development of crop straw resources in Northeast China (东北地区作物秸秆资源综合利用现状与发展分析). *Journal of Agricultural Machinery*, Vol.48, pp. 1-21, Beijing/China.

[15] Yang, R., Wang, Z., Shang, S., (2020). Experiment on Removing Soil Device with Spring Tooth of Peanut Combine Harvester (花生联合收获机弹齿式去土装置设计与性能试验). *Journal of Agricultural Machinery*, Vol.51, pp. 109-117, Beijing/China.

[16] Zhang, H., Liu, X., Wu, H., Xu, X., Xu., D., (2019). Suspended silage round bundle machine (悬挂式青贮圆捆包膜机的研究). *Agricultural mechanization research*, Vol.41, pp. 159-164, Heilongjiang/China.

[17] Zhang, X., Wang, Z., Shen, M., Bai, H., Ta, N., (2021). Analysis of the yield and comprehensive utilization of crop straw in China (中国农作物秸秆产量及综合利用现状分析). *Journal of China Agricultural University*, Vol.26, pp. 30-41, Beijing/China.

[18] Zhang, Y.I, Li, X., Wang, J., Li, X., An, T., (2017). The effect of the coating number on the quality of sweet sorghum silage (裹包层数对甜高粱青贮饲料品质的影响). *Acta Agrestia Sinica*, Vol. 25, pp. 670-674, Beijing/China.

[19] Zhao, G., Liu, X., Wu, H., Chen, A., Zhang, Q., Song, Q., Xing, W., Zhang, H., (2024). Design and Test of Key Components of Corn Straw Baler Conveyor (玉米秸秆打捆机输送装置关键部件的设计与试验). *Journal of Agricultural Mechanization Research*, Vol. 47, pp. 82-87, Heilongjiang/China.